Theoretical study of electronic and transport properties of PPy–Pt(111) and PPy–C(111):H interfaces

2010 J. Phys.: Condens. Matter 22 045003

(http://iopscience.iop.org/0953-8984/22/4/045003)

J. Phys.: Condens. Matter **22** (2010) 045003 (10pp) doi:10.1088/0953-8984/22/4/045003

Theoretical study of electronic and transport properties of PPy–Pt(111) and PPy–C(111):H interfaces

Wojciech Kamiński[1,2], **Vit Rozsíval**[2] **and Pavel Jelínek**[2]

[1] Institute of Experimental Physics, University of Wrocław, plac Maksa Borna 9, PL-50-204 Wrocław, Poland
[2] Institute of Physics, Academy of Sciences of the Czech Republic, Cukrovarnická 10, CZ-162 53 Prague, Czech Republic

E-mail: kamien@ifd.uni.wroc.pl

Received 1 July 2009, in final form 25 November 2009
Published 5 January 2010
Online at stacks.iop.org/JPhysCM/22/045003

Abstract

We present a first-principles study of promising hybrid organic–inorganic interface systems consisting of a polypyrrole (PPy) chain sandwiched between metallic Pt(111) or hydrogen-terminated diamond C(111):H electrodes. We combine *ab initio* density-functional-theory total energy calculations, Green's function approach and the complex band-structure method in order to determine electronic and transport properties of those organic–semiconductor/metal (semiconductor) interfaces. We analyze one- and multi-bond nanocontact formation including structural modification (H desorption) as well as PPy length dependence. For selected ground state configurations of the considered interface systems we study their energetics and structural properties. Through the analysis of the local density of states, in particular isosurfaces of the charge density, the mechanism of the charge transfer and the charge neutrality levels are determined. The voltage dependence of the electrical conductance and the I–V characteristics are compared to the transport properties based on the complex band-structure method. The obtained results support recent experiments, where PPy nanowires are formed via electrochemical synthesis and placed between platinum or diamond microelectrodes.

(Some figures in this article are in colour only in the electronic version)

1. Introduction

One of the main goals of nanotechnology is to build an electronic device using individual molecules. To accomplish this challenge, the control and understanding of electron transport through molecules attached to electrodes is crucial. Substantial progress in the measurement and modeling of transport in atomic-scale junctions has been made over the past decade [1–7]. Experimental techniques achieved the status when controlled and well-defined contact between molecules and electrodes can be established [8–11]. However, for wider prospective technological applications, more theoretical and experimental effort is required for a detailed microscopic understanding of the charge transport through molecular junctions.

Over the last decade, the interest in organic materials has significantly increased. It is due to the vast spectrum of their use in electronic and microelectronic devices, mostly as very cheap screens, thin-film transistors and photovoltaic cells [12]. There are many different kinds of conjugated polymers, but we focus on polypyrrole (PPy), which is one of the most stable [13]. Individual PPy nanowires exhibit actuation behavior [14, 15] and therefore can potentially be used for constructing nanoscale components essential for nanoelectromechanical systems and nanorobots. PPy is a semiconducting polymer from the rigid-rod polymer host family. It is made up by oxidation and polymerization of the pyrrole-heterocyclic aromatic organic compound with the formula C_4H_5N, also known as pyrrole (Py). The experimental HOMO–LUMO gap of PPy is 1.3–3.2 eV, depending on the

method of preparation (for details, see, e.g., [16–19]). Due to its chemical stability, high conductivity upon doping and nonlinear optical properties, PPy is among the most widely experimentally studied conjugated organic polymers.

Combining the advantages of PPy and inorganic materials results in promising hybrid organic–inorganic functional devices. Nowadays, one of the main challenges is to assemble and connect molecules and inorganic materials into functional systems on a microscopic scale in an easy and reproducible way [1, 20]. Merging of PPy molecules with inorganic materials, such as semiconducting hydrogen-terminated diamond [21, 16] or platinum microelectrodes [22–24], has already focused experimental attention. However, theoretical studies of such interface systems, although very important for further device development, are sill lacking. First-principles calculations, based on density-functional theory (DFT), can provide a significant physical insight into the real mechanisms of the contact formation, and consequently into the electronic, as well as transport, properties of the resulting organic–semiconductor/metal (semiconductor) interfaces.

From this perspective, we have performed an extensive set of first-principles molecular dynamics simulations of the interaction between a PPy nanowire and C(111):H (hydrogen-terminated diamond) surface (PPy–C:H organic–semiconductor/semiconductor interface) or Pt(111) surface (PPy–Pt organic–semiconductor/metal interface) to investigate the formation of individual contacts responsible for the transport properties.

A brief outline of this paper follows. In section 2, we describe details of the theoretical techniques used to investigate the atomic and electronic structure of molecular heterojunctions. Here, we also propose atomistic models of the studied electrode–molecule interface system. Section 3 provides a discussion of the electronic and atomic structures of an infinite PPy and their change with respect to molecular Py. The structural and electronic properties of the considered junctions, obtained from DFT calculations, are discussed in section 4. In section 5, we discuss the transport properties of individual atomic configurations using the complex band-structure technique and Green's function method. Finally, in section 6, we summarize our results.

2. Methods

2.1. First-principles simulations

Our calculations, performed using the FIREBALL code [25–28], are based on DFT with a local-orbital basis. This code is designed to deal with large-scale simulations and offers a very favorable accuracy-to-efficiency balance, provided that the basis set is carefully chosen [29]. The calculations presented in this paper are performed within the local density approximation (LDA) for the exchange–correlation functional [30].

In FIREBALL, the wavefunctions of valence electrons are expanded in the basis of so-called FIREBALL orbitals [25, 28], i.e. a set of strictly localized pseudoatomic orbitals, which are exactly zero for distances larger than the cutoff radius R_C. A very important point of our method is a proper choice of the basis and the cutoff radii that gives consistent results, not only for the electronic structure but also for the structural properties of the studied system. Thus, several tests have been performed to optimize the local-orbital basis set, yielding a good description of the structural and electronic properties of PPy chain either Pt or C:H electrodes. We have used the following optimized basis set of numerical atomic orbitals [25, 29]: ss* for H, spd* for C, spd* for N and spdd* for Pt. The cutoff radii (in a.u.) of those orbitals are: 3.8 (s), 3.8 (s*) for H, while (4.5, 4.5, 5.4), (3.6, 4.1, 5.2) and (4.6, 5.8, 4.2, 4.2) for orbitals of C, N and Pt, respectively.

2.2. Modeling of interface systems

The PPy molecular nanowire is sandwiched between two electrodes with (111)-oriented surface planes. This is realized by using a supercell approach with the unit cell comprised of the PPy nanowire and one electrode, as shown in figure 1. We have also imposed periodic boundary conditions in the direction perpendicular to the surface. The electrodes have been modeled by slabs (four Pt layers for metallic electrode and five C double layers for C:H) with a 3×3 surface unit cell for C:H and a 4×4 cell for Pt.

In our calculations, we have investigated PPy nanowires with 6–13 Py rings. Results obtained for PPy nanowires build up by 12 and 13 Py rings show no significant differences, either for metal (Pt) or semiconducting (C:H) electrodes, hence the influence of the odd or even number of Py rings in the chain is negligible. Moreover, the electronic structure in the middle of a PPy chain of that length, sandwiched between electrodes, reproduces fairly well the electronic properties of an infinite PPy chain. Thus, we have concluded that the length of a PPy nanowire built of 12/13 Py rings is sufficient to model this kind of interface system.

The assumed size of the surface unit cells of the considered slabs has been chosen so that the PPy nanowires from the neighboring cells are virtually noninteracting, while the total number of atoms in the unit cell (234 for PPy–Pt and 314 for PPy–C:H) remains reasonable from the computational point of view. Nevertheless, the influence of the size of the surface unit cell has been tested for the PPy–Pt interface and almost identical results have been obtained for a 3×3 and a 4×4 cell.

To study the contact formation, in the first step we composed the system of the relaxed C:H (Pt) symmetric slab and the PPy chain. Having in mind the previously calculated bond length of the C–Pt (C–C) dimer we guess the size of the unit cell in the longitudinal direction which should be close to the equilibrium one. The contact formation (depending on its one- or multi-bond nature) is allowed by an additional removal (if necessary) of some hydrogen atoms from the system. Experimentally, the H-termination is substituted by the PPy molecules during the electrochemistry [21]. Since we are focused on the transport properties which are dependent mainly on the nature of the bonding of the PPy chain to the electrodes, we have studied the interfaces without any dehydrogenation processes; the H atoms, if necessary, are removed before

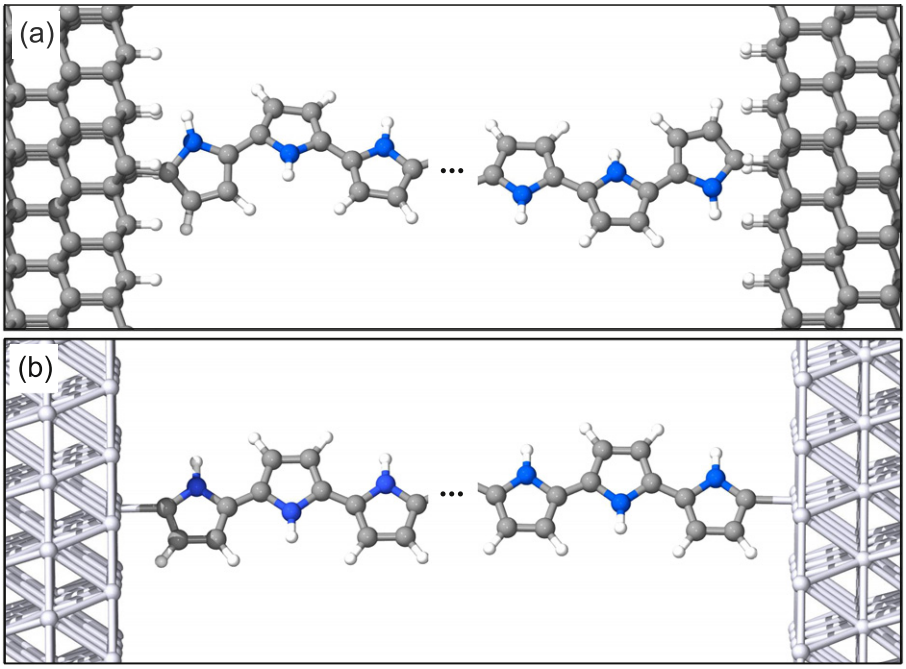

Figure 1. Schematic illustration of the unit cell used in calculations. The PPy molecular nanowire is placed between hydrogen-terminated diamond (a) or platinum (b) electrodes. Only parts of the PPy chains closest to the electrodes are shown.

the simulation starts. This way we set individual PPy–C:H (PPy–Pt) interfaces composed of a PPy nanowire sandwiched between two (111)-oriented C:H (Pt) electrodes. Then, for each of these initial configurations, we have performed the total energy calculations by changing the size of the unit cell by 0.2 Å in the longitudinal direction. For each new size of unit cell, we have relaxed the system according to the maximum force tolerance set up to 0.05 eV $Å^{-1}$ and the total energy variation less than 0.0001 eV. The configuration with the lowest energy is considered as the ground state configuration. The surface Brillouin zone has been sampled by a $8 \times 8 \times 1$ ($4 \times 4 \times 1$) Monkhorst–Pack [31] grid for the PPy–C:H (PPy–Pt) interface system, which yields 8 (5) irreducible special k-points. Convergence tests with denser k-point sampling show negligible changes to the energies and the structural properties.

3. From Py to PPy

As the first step, we have performed the structural optimization of a Py molecule obtaining a HOMO–LUMO gap of 4.95 eV. Afterward, we have modeled an infinite PPy chain using a supercell approach with the unit cell containing two Py rings. Structural relaxation is performed and the lattice parameter in the longitudinal direction is optimized (7.025 Å) to obtain the minimum total energy of a PPy nanowire. The obtained structure of the relaxed infinite PPy chain is shown in figure 2(a).

Only small structural differences of the PPy geometry are found with respect to the Py molecule, namely, a decrease of the N–C bond length from 1.43 Å to 1.40 Å as well as the double C=C bond from 1.35 Å to 1.34 Å, and an increase of the single C–C bond length from 1.43 Å to 1.45 Å. Accordingly, changes of internal angles within Py rings are less than $\pm 2°$. The obtained structural parameters for the PPy chain are in good agreement with the other theoretical study [18]. The calculated density of states of an infinite PPy chain (with 32 k-points sampling the Brillouin zone) shows the semiconducting character of the PPy nanowire with a kind of HOMO–LUMO gap of 2.08 eV (see figure 2(b)) which is in good agreement with experimental evidence [16–19]. Electronic states of the PPy within the energy range of -2.0 to 2.0 eV (see figures 2(c) and (d)) are out-of-plane π molecular orbitals maintaining the spatial distribution of the HOMO and LUMO of the Py molecule, with almost the same contributions of atomic orbitals.

4. Structural and electronic properties of PPy–C:H (PPy–Pt) interfaces

4.1. Contact formation

As follows from our simulations, the PPy nanowire does not adsorb on the clean hydrogen-terminated diamond C:H surface. Thus, we modeled a system in which some H atoms are removed before simulations. The one-bond (two-bond) contact is formed when one (two) H atoms are removed from both the C:H surface and the last PPy ring. The one-bond contact formation in the case of PPy–Pt is allowed when just one H atom at the end of the PPy molecular nanowire is removed, whereas two H atoms need to be removed from the end of the PPy nanowire to allow the formation of multiple C–Pt bonds.

For both studied systems, i.e. the PPy–C:H and PPy–Pt interfaces, the one- and multi-bond contact formation is considered. Consequently, presented results concern four

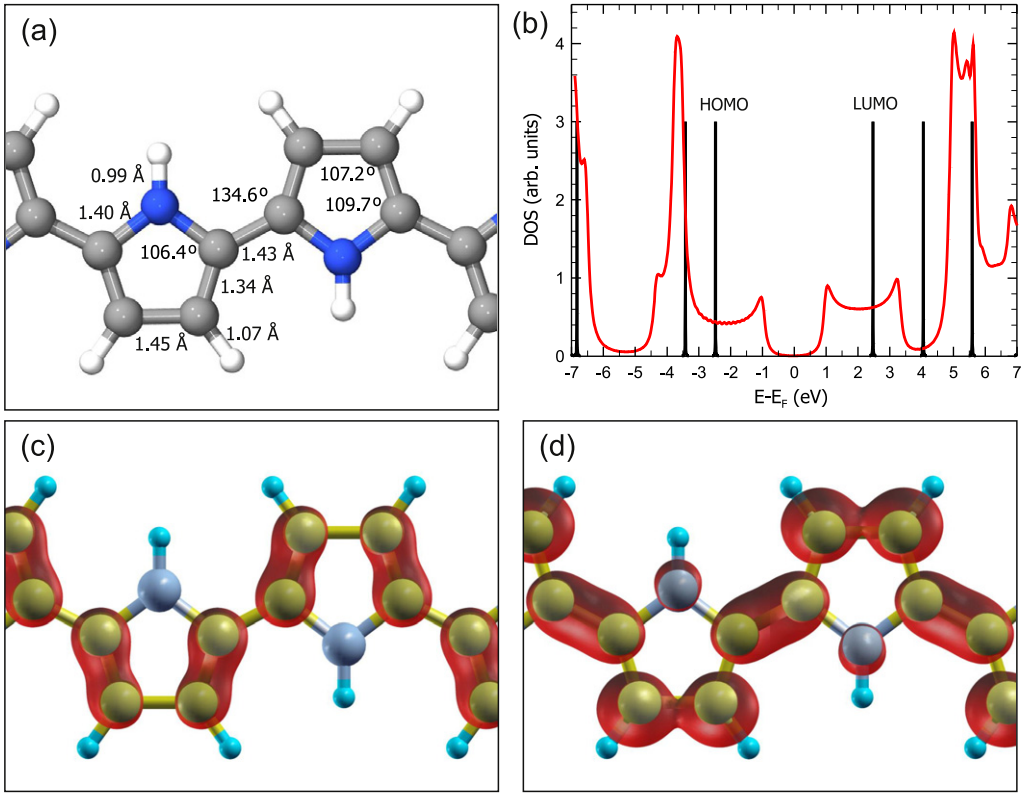

Figure 2. (a) Sketch of the chain structure of PPy with main structural parameters indicated. Color code for atoms: hydrogen (white), nitrogen (blue/dark-gray) and carbon (light-gray). (b) Density of states of an infinite PPy chain (red/gray line) with a bandgap of 2.08 eV and molecular orbitals of an isolated Py monomer (black vertical lines) with the HOMO and LUMO being separated by 4.95 eV. Isosurfaces of the electronic charge density of PPy (corresponding to the value of $0.02e$ Å^{-3}) integrated over the energy range −2.0–0.0 eV (c) and 0.0–2.0 eV (d) (all energies are relative to the Fermi level).

Table 1. The number n of H_2 molecules, the binding E_b and the interaction E_{int} energy (per interface), the charge transfer Δq from the PPy nanowire to the electrode, and the CNL for the PPy–C:H and PPy–Pt interfaces.

	n	E_b (eV)	E_{int} (eV)	Δq (e^-)	CNL (eV)
PPy–C:H 1-bond	2	−1.26	6.15	−0.11	−0.59
PPy–C:H 2-bond	4	−4.43	10.89	−0.20	−0.65
PPy–Pt 1-bond	1	1.00	6.49	0.06	0.02
PPy–Pt 3-bond	2	0.87	10.67	0.05	0.04

different structures: one- and two-bond contacts for the PPy–C:H interface and one- and three-bond contacts for the PPy–Pt system. For each of them, the structural and electronic properties have been analyzed, and the binding and the interaction energies, the charge transfers and the charge neutrality levels (CNL) are collected in table 1.

4.2. Structural modification due to contact formation

For all studied cases the geometry of the electrodes is practically unaffected by the interaction with PPy nanowires, while significant modification of the Py rings in the contact region is observed. The detailed structural data are given in figures 3(a)–(d) for each considered contact. The Py units closest to the electrode are slightly rotated with respect to the rest of the nanowire as a consequence of the contact formation. Accordingly, torsion angles between the rings in the contact region are modified as well (see, e.g., figure 3(a)). Modification of the bond length in the PPy ring closest to the contact, where most pronounced deformation of the PPy chain occurs, is less than 5% as compared to the infinite PPy chain. All outermost C atoms of the PPy nanowire, involved in the formation of interface bonds, are located on top sites, except for one C atom (in the three-bond PPy–Pt case) which forms two bonds with Pt surface atoms in a bridge position.

4.3. Binding and interaction energies

In this section, we aim to discuss the energy balance of the PPy–C:H and PPy–Pt interfaces. Here, the binding energy E_b is defined as a difference between the total energy of the whole relaxed system before and after contact formation, divided by two, since we have two interfaces in our model:

$$E_b = [(E_{PPy} + E_{slab}) - (E_{con} + n{\cdot}E_{H_2})]/2, \qquad (1)$$

where E_{PPy} and E_{slab} are the total energies of the PPy molecule and electrode slab before the contact formation, respectively, whereas E_{con} is the total energy of the formed contact and E_{H_2} is the energy of a single H_2 molecule. The number n of H_2 molecules formed by dehydrogenated H atoms depends on a

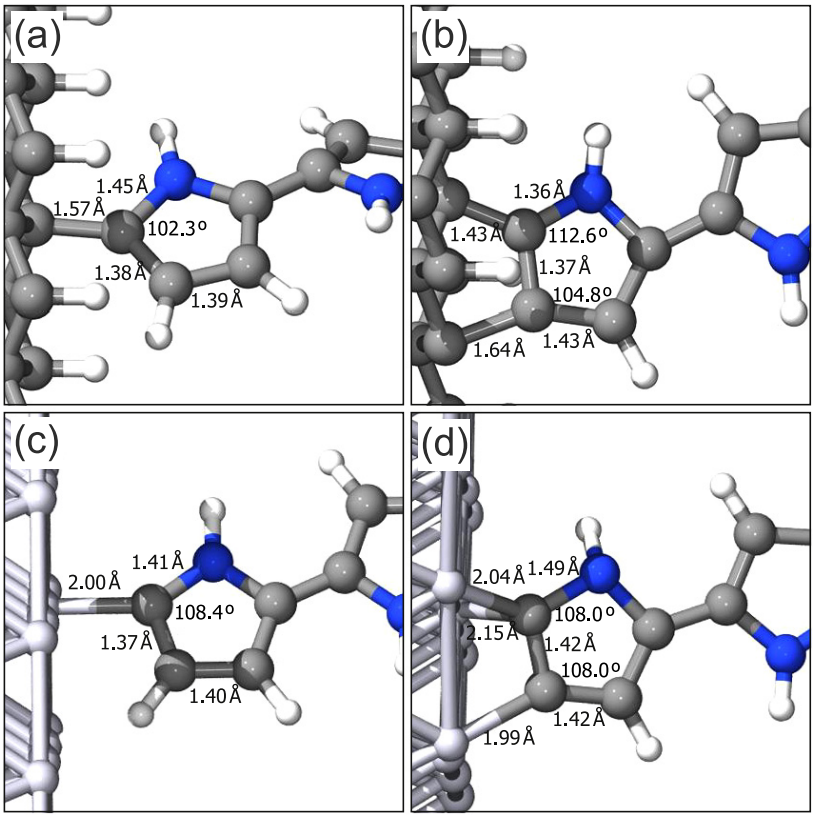

Figure 3. Side views of the contact regions of different considered interfaces with detailed structural parameters indicated. (a) and (b): the PPy–C:H one- and two-bond contact, respectively. (c) and (d) the PPy–Pt one- and three-bond contact, respectively.

particular bonding situation. In our nomenclature, a positive value of E_b indicates an exothermic process.

The binding energies for different systems are summarized in table 1. According to our simulation, formation of PPy–Pt interfaces is an energetically favorable process (by ∼1 eV per interface) for both one- and multi-bond cases. The contact formation of PPy–C:H interfaces requires extra energy since a negative value of E_b indicates a nonspontaneous character of this reaction. Moreover, the calculated values of E_b for PPy–C:H systems indicate that the one-bond PPy–C:H contact is much more favorable compared to the two-bond contact which requires three times more energy to be created (see table 1).

In addition, to determine the character of bonds formed between the molecule and the electrodes, we have introduced the interaction energy per interface E_{int} using the formula

$$E_{int} = [(E_{slab-H} + E_{PPy-H}) - E_{con}]/2, \qquad (2)$$

where E_{slab-H} is the energy of the electrode slab and E_{PPy-H} is the energy of the PPy nanowire, both without H atoms which have been removed to allow the contact formation.

The interaction energies—computed according to the above formula—seem not to depend on whether the electrode is metallic (Pt) or semiconducting (C). The interaction energy is about 6 eV for one-bond interfaces and nearly twice this value (∼11 eV) for multi-bond contacts. We want to point out here that we do not include any dehydrogenation in the process of contact formation, because H atoms are removed during modeling of the interface system. Thus, the number of atoms in the interface system is a sum of atoms in the slab and the PPy nanowire. Magnitudes of the interaction energies indicate the presence of strong covalent bonds at all considered interfaces.

4.4. Charge transfer and CNL

The PPy nanowire does not stay neutral once placed between metal or semiconductor electrodes. For the PPy–Pt system a charge transfer occurs from the PPy nanowire to an electrode, which agrees with recent experiments [22]. The amount of charge transferred to the Pt slab shows no significant dependence on the type of contact formed, being 0.06 electrons for a one-bond and 0.05 electrons for a three-bond interface. This differs from the case of semiconductor electrodes, where the charge transfer occurs in the opposite direction (from an electrode to the PPy nanowire) and is doubled for the two-bond contact. The charge transfer between electrodes and the PPy nanowire can be described by CNL [32] of the PPy molecule. The CNL position indicates the energy at which the organic molecule in the interface system is neutral. Calculated values of CNL (with respect to the Fermi level) are collected in table 1 and shown as vertical solid lines in figures 4(a) and (b) and 6(a) and (b). Our results are in good agreement with previous experimental work [16, 33], where the charge transfer from covalently bound PPy to diamond has been indicated by Kelvin force microscopy.

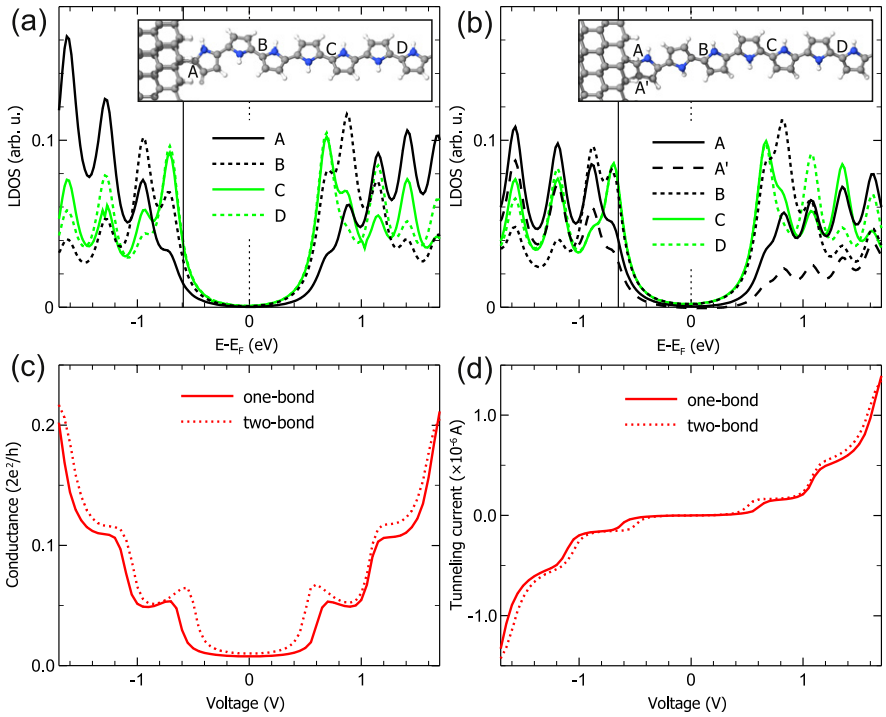

Figure 4. Density of states projected on different carbon atoms of the PPy nanowire for one-bond contact (a) and for two-bond contact (b) at the PPy–C:H interface. Dotted and solid vertical lines indicate E_F and CNL, respectively. Insets in (a) and (b) show the position of carbon atoms for which the LDOS is plotted. (c) Electrical conductance of PPy–C:H contacts for one-bond contact (solid red line) and two-bond contact (dotted red line). (d) Tunneling current for the cases considered in (c).

4.5. Electronic properties

The electronic structure of the studied interfaces is analyzed through local density of states (LDOS) projected on selected atoms of the PPy nanowire. We have chosen the carbon atom at the end of the PPy nanowire (A), through which the contact is formed (for the multi-bond contact, one more carbon atom, denoted by A′, is considered), and other carbon atoms (B, C, D), each of them further by two PPy rings from the interface (see the insets in figures 4 and 6).

Both one- and two-bond PPy–C:H interfaces (see figures 4(a) and (b), respectively) are semiconducting with a significant gap decrease from 2.08 eV for an infinite PPy to about 1.3 eV (in the middle of the PPy nanowire) for the PPy–C:H interface system. This is clearly visible in the LDOS projected on carbon atoms (C, D) located in the region between electrodes. As we get closer to the contact, the influence of the semiconducting electrode results in the gap broadening up to 2 eV at the outermost carbon atom (A). The LDOS for the one- and two-bond PPy–C:H interfaces does not show any pronounced differences. The CNL of the PPy nanowire also differs insignificantly (see table 1 and vertical lines in figures 4(a) and (b)), but the charge transfer from the PPy nanowire to the diamond substrate is two times bigger for the two-bond contact.

Spatial distributions of the electronic charge density in the vicinity of the gap are shown in figures 5(a)–(d). There are presented isosurfaces of the electronic charge density integrated over the energy range of 1 eV below (figures 5(a) and (c) for one- and two-bond contacts, respectively) or 1 eV above the Fermi level (figures 5(b) and (d) for one- and two-bond contacts, respectively). All isosurfaces correspond to the value of $0.01e$ Å^{-3}. We see a small modification of the molecular HOMO and LUMO just in the contact region (within the two Py rings closest to the electrode), as compared to the charge density distribution for an infinite chain (see figures 2(c) and (d)). A lower electronic density for those atoms is interpreted as the gap opening near the electrode and is consistent with the LDOS presented in figure 4.

In the case of the PPy–Pt system we have found substantial modification of the electronic structure of C atoms at the interface. In particular, new induced states appear within the gap of the PPy due to a strong hybridization with metal electrons. The effect of the PPy gap decrease is also present in the case of metallic electrodes. For one- and three-bond contacts at the PPy–Pt interface, the gap in the middle of the PPy nanowire is about 1.6 eV (see atoms C and D in figures 6(a) and (b)). As a result of the new electronic states induced within the gap of the PPy nanowire, a strong modification of the LDOS is observed for the Py rings closest to the contact. This is illustrated by the LDOS projected on carbon atoms forming the metal–molecule interface: atom A for one-bond contact (figure 6(a)) and atoms A and A′ for three-bond contact (figure 6(b)). For the one-bond contact, the Fermi level of the system coincides with the bottom of the PPy gap (HOMO-like orbitals of the outermost Py ring cross the Fermi level), while for the three-bond contact, although new electronic states are also introduced within the PPy gap region, the Fermi level remains in the middle of the PPy nanowire gap.

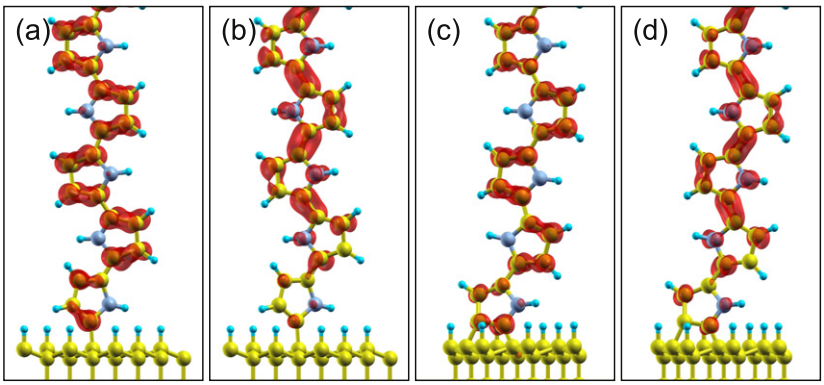

Figure 5. Isosurfaces of electronic charge density corresponding to the value of $0.01e$ Å^{-3} and integrated over the energy range -1.0–0.0 eV ((a) and (c)) or 0.0–1.0 eV ((b) and (d)) for the one-bond ((a) and (b)) or the two-bond ((c) and (d)) contact at PPy–C:H interfaces.

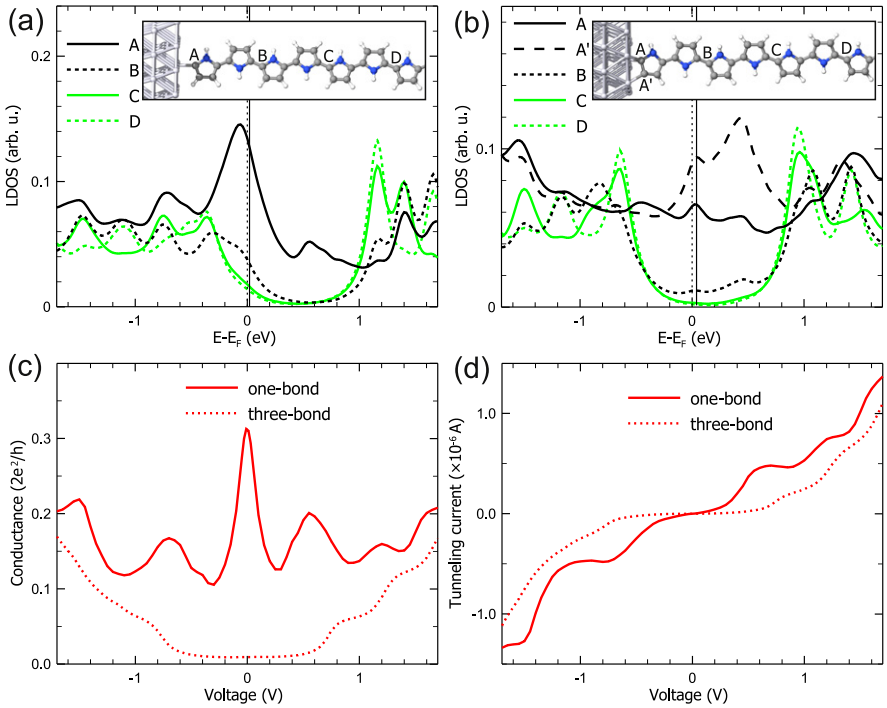

Figure 6. Density of states projected on different carbon atoms of the PPy nanowire for one-bond contact (a) and for three-bond contact (b) at the PPy–Pt interface. Dotted and solid vertical lines indicate E_F and CNL, respectively. Insets in (a) and (b) show the position of carbon atoms for which the LDOS is plotted. (c) Electrical conductance of PPy–Pt contacts for one-bond contact (solid red line) and two-bond contact (dotted red line). (d) Tunneling current for the cases considered in (c).

We have also examined spatial distributions of the electronic charge density for the PPy–Pt system. The electronic charge density integrated over the energy range of -0.2–0.0 eV and 0.0–0.2 eV with respect to the Fermi level is shown as isosurfaces corresponding to the density of $0.01e$ Å^{-3}. Figure 7 shows isosurfaces for states below (a) and above (b) the Fermi level for the case of one-bond contact, while those for the three-bond contact are presented in figures 7(c) and (d), respectively. New electronic states induced within the PPy gap for the one-bond PPy–Pt interface (see the LDOS for atom A in figure 7(a)) have a spatial distribution similar to the former HOMO-like states of an infinite PPy chain (see figure 2(a)). In the case of three-bond contact, electronic states within the PPy gap are mainly located at carbon atoms of the two PPy rings closest to the contact. For both one- and three-bond PPy–Pt interfaces, the analysis of the density of states projected on particular orbitals of the C atoms forming contacts (not shown) indicates that those states gain a character of σ-symmetry.

5. Transport properties of PPy–C:H (PPy–Pt) interfaces

Electron transport through a molecular junction is generally determined by two key factors: (i) the electronic structure of molecules and (ii) the nature of contacts between electrodes and molecules. The first factor can be characterized in an elegant way by the complex band-structure methods [34, 35], within which the electron transport through individual

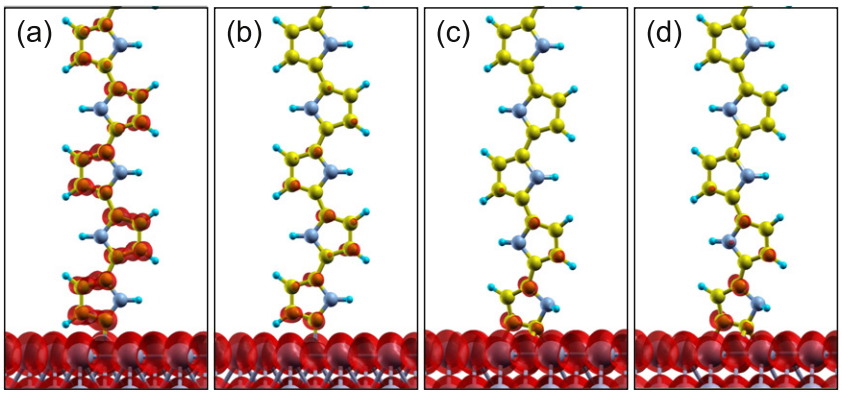

Figure 7. Isosurfaces of electronic charge density corresponding to the value of $0.01e$ Å^{-3} and integrated over the energy range −0.2–0.0 eV ((a) and (c)) or 0.0–0.2 eV ((b) and (d)) for the one-bond ((a) and (b)) or the three-bond ((c) and (d)) contact at PPy–Pt interfaces.

molecules is characterized by a single parameter β. The second factor requires elaborate theoretical simulations, taking properly into account atomic relaxation of the contact, as well as the Fermi level alignment between a molecule and electrodes, which induces a charge transfer and subsequent formation of a dipole layer at the interface (for details, see, e.g., [32]).

Table 2. Comparison of the conductance calculated by the complex band-structure method G^{CB} and Green's function method G^{GF} for PPy–Pt interfaces. l_{eff} is the molecule length at which $G^{\mathrm{CB}} = G^{\mathrm{GF}}$.

	E_{F} (eV)	β (Å^{-1})	G^{CB} (μS)	G^{GF} (μS)	l_{eff}
PPy–Pt 1-bond	−3.81	0.20	0.0083	24.10	5.81
PPy–Pt 3-bond	−3.67	0.22	0.0033	0.72	21.26

5.1. Complex band-structure method

Electron transport through single molecules with a well-defined HOMO–LUMO gap is usually driven by a tunneling mechanism. In a molecular junction, the tunneling current becomes exponentially small for long molecules $\exp^{-\beta l}$, where l is the distance between two electrodes and the exponential decay parameter β describes the tunneling of electrons through the molecular gap. The parameter β is just the key quantity that characterizes the transport process through a molecule which is usually determined by the complex band-structure method [34, 35].

It is well known that the LDA approximation underestimates, in particular in molecular systems, the bandgap. The GGA approximation could improve the binding energy, but does not correct the problem of the bandgap. However, the underestimating effect of the LDA is compensated in our calculations because we use a basis set of FIREBALL orbitals. Thus, the HOMO–LUMO gap of 2.08 eV obtained for a PPy infinite chain is in good agreement with the experimental value of 1.3–3.2 eV [16–19]. Apart from the well-known bandgap problem [32, 36, 37], there are no spurious crossing level effects [38] requiring extra many-body corrections [39]. Here, we compare results given by complex band-structure and Green's function methods only for the PPy–Pt interface system due to the fact that, for this system, the Fermi energy is well defined. The band structure of an infinite PPy molecular wire is shown in figure 8(a) together with the complex band structure 8(b).

A rough estimation of the conductivity of the PPy for a given energy can be made once we know the energy dependence of $\beta(E)$ from the complex band structure. To compare with the more sophisticated Green's function method we consider the energy E corresponding to the Fermi level of the metal/molecule interface system. We approximate the conductance (G) at E_{F} for the molecule of length l ($l \approx 46$ Å) by the formula

$$G(E_{\mathrm{F}}) \approx G_0 e^{-\beta(E_{\mathrm{F}})\cdot l}, \tag{3}$$

where G_0 is the conductance quantum unit $2e^2/h$ ($G_0 = 77\ \mu$S).

In table 2 we summarized the conductance calculated from the complex band-structure method and Green's function method (discussed later in detail). The main difference comes out from the fact that the complex band-structure method does not take into account any local changes of the electronic structure in the molecular wire due to induction of new states within the molecular gap near the Fermi level. Therefore, the effective tunneling distance l_{eff} is shorter than the actual molecular wire length l. This kind of effect should be carefully considered in a realistic estimation of the electron transport through molecular wires using the complex band-structure method.

5.2. Green's function method

We have also calculated transport properties for the ground state of the PPy–C:H (PPy–Pt) interface structures from the tight-binding Hamiltonian using Green's function techniques [40, 41] implemented in the FIREBALL code (for details, see, e.g., [42, 40, 43]).

The interface system for calculating transport properties is modified by adding an identical electrode slab to the other side of the PPy nanowire and removing the periodic boundary condition in the direction perpendicular to the surface (longitudinal direction). Thus, in the unit cell we

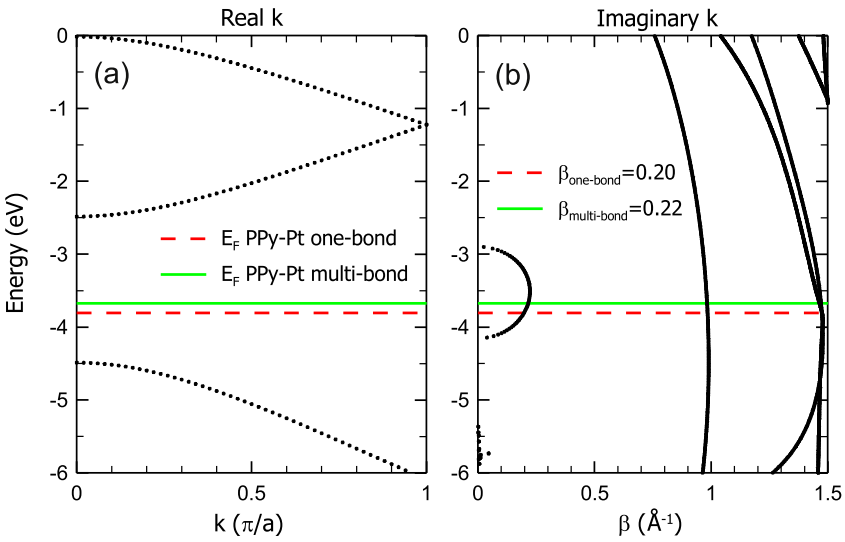

Figure 8. Complex band structure of a PPy molecular nanowire: a band structure with real k (a) and the decay parameter β versus energy (b). Two horizontal lines indicate the position of the Fermi level for the PPy–Pt system with one bond (red dashed line) and three bonds (green solid line) established between the molecule and the surface atoms.

have the PPy molecular nanowire sandwiched between two electrodes—metal (Pt) or semiconducting (C:H). To compute the conductance or tunneling current we divide this unit cell into two subsystems I and II [40]: one electrode and a half of the PPy nanowire on the one side as subsystem I and the rest of the PPy chain and the other electrode as subsystem II.

The voltage dependences of the electrical conductance calculated for all studied systems are shown in figures 4(c) and 6(c) for PPy–C:H and PPy–Pt interfaces, respectively. At the PPy–C:H interfaces the conductance shows very similar behavior for one- and two-bond contacts, although a clearly seen bandgap is wider for one-bond contact (1.4 versus 1.2 eV). For higher voltages the PPy–C:H interface becomes conducting and the conductance dependence shows a kind of peak due to the fact that the electronic structure of a finite PPy nanowire remains discrete. The only difference is that the maxima reflecting molecular orbitals of the PPy nanowire for a two-bond contact are slightly shifted to lower bias (see the red dotted line versus the red solid line in figure 4(c)). Consequently, the calculated tunneling current through PPy–C:H interfaces, shown in figure 4(d), exhibits very similar voltage dependence for one-bond as well as two-bond contacts.

The transport properties of the PPy–Pt system are analyzed through voltage dependence of the conductance (see figure 6(c)) and the tunneling current (see figure 6(d)). This interface shows remarkable changes according to the local bonding arrangement between electrodes and molecular wire. In particular, the one-bond contact has large conductivity near the Fermi level ($\sim 0.3G_0$) due to the fact the former HOMO of the PPy chain is pinned to the Fermi level. On the other hand, the transport properties of the three-bond PPy–Pt system (dotted red lines in figures 6(c) and (d)) near the Fermi level are driven by tunneling processes, similar to the case of PPy–C:H interfaces. Therefore, three-bond contact PPy–Pt interface is semiconducting, with a bandgap of $\sim$1.4 eV, opposite to the one-bond contact PPy–Pt interface which is metallic.

6. Conclusions

We have carried out first-principles simulations of hybrid organic–semiconductor/metal (semiconductor) interface systems in order to understand the structural and electronic properties that are responsible for the electronic transport of such interfaces. To achieve this goal, we have first examined both a single Py molecule and an infinite PPy chain. Then, we have studied the process of interface formation in the PPy–C:H (PPy–Pt) systems. We have found out that the contacts are formed only when some of the H atoms are previously removed from the interface. No influence of the odd or even number of Py rings within the PPy nanowire is found for PPy chains longer than 12 Py rings.

The calculated binding energies show that the PPy–Pt interfaces are energetically more stable than the PPy–C:H contacts. In addition, we have introduced the interaction energy to reveal the bonding character between the PPy nanowire and the electrode. The obtained values of the interaction energy ($\sim$6 eV per bond) points out a covalent character of the bonds formed at the one- and multi-bond contacts, for the PPy–Pt as well as the PPy–C interfaces. The covalent bonding of PPy to C:H agrees very well with recent AFM-scratching measurements [16].

Electronic structures of the considered interfaces analyzed through the LDOS and the isosurfaces of the electronic charge density show that only the one-bond PPy–Pt interface system is metallic, while the one- and two-bond PPy–C:H interfaces as well as the three-bond PPy–Pt interface are semiconducting. For the PPy–C:H interface the CNL is located below the Fermi level, so the transfer of electrons occurs from an electrode to the PPy molecular nanowire, which is in contrast to the PPy–Pt case where the CNL is located above the Fermi level. The value of the charge transfer ($\sim 0.05e^-$) does not depend on the number of formed bonds for the PPy–Pt interface, but it is two times bigger for the two-bond contact than for the

one-bond contact in the case of the PPy–C:H interface. The gap decrease from 2.08 eV for an infinite PPy chain to ∼1.3 (1.6) eV is observed in the middle of the PPy chain for the PPy–C:H (PPy–Pt) interface system. Significant modification of the electronic structure of the PPy chain in the contact region (i.e. within the outermost Py rings) is observed. This effect depends on the electrode (Pt or C:H) and the number of bonds at the interface. The gap broadening occurs for the PPy–C:H while for the PPy–Pt new electronic states are induced within the gap. In particular, the one-bond PPy–Pt interface becomes metallic since the former molecular HOMO of the PPy chain crosses the Fermi level. This result matches up very well with experimental evidence that the platinum Fermi level is ∼0.5 eV below HOMO of PPy [22].

Finally, we have studied the transport properties of the PPy–C:H (PPy–Pt) with two different methods: the complex band-structure method and Green's function technique. We found that, for realistic estimation of the conductance via the complex band-structure method, the tunneling length should be corrected, namely, if new induced states in the molecular gap are formed. We found that the conductance of the PPy–Pt system near the Fermi level is sensitive to the character of the bond formed at the interface.

In conclusion, our simulations showed the importance of the dehydrogenation process on the formation of the interface between molecule and electrode and its transport properties. Elimination of terminating hydrogen atoms allows the formation of the covalent bond between the molecular chain and the electrode which enhances both mechanical stability and the electron transport of the contact. In the case of the PPy–Pt interface, we have observed a strong dependence of the Fermi level alignment on the number of carbon atoms involved in the contact formation. The presented simulations provided a detailed information about the electronic structure of the molecular junction. It can help to propose appropriate dopants to achieve the desired electronic properties. We have found that the electron transport through the PPy molecular chain is driven by the tunneling process. Therefore, a pertinent doping of both molecular wire and diamond surface would enhance the electron transport. However, simulations addressing the doping effect are beyond the scope of this paper.

Acknowledgments

We are grateful to Dr B Rezek, Professor O F Sankey and Dr M H Lee for inspiring discussions. This work has been supported by the GAAV grant no. KAN400100701, GACR no. 202/09/0545 and COST P19-OC09028.

References

[1] Cui X D, Primak A, Zarate X, Tomfohr J, Sankey O F, Moore A L, Moore T A, Gust D, Harris G and Lindsay S M 2001 *Science* **294** 571
[2] Lindsay S M and Ratner M A 2007 *Adv. Mater.* **19** 23–31
[3] Kiguchi M, Tal O, Wohlthat S, Pauly F, Krieger M, Djukic D, Cuevas J C and van Ruitenbeek J M 2008 *Phys. Rev. Lett.* **101** 046801
[4] Jelínek P, Pérez R, Ortega J and Flores F 2006 *Phys. Rev. Lett.* **96** 046803
[5] Agrait N, Yeyati A L and van Ruitenbeek J M 2003 *Phys. Rep.* **337** 81–279
[6] Paulsson M, Frederiksen T and Brandbyge M 2005 *Phys. Rev.* B **72** 201101
[7] Imry Y and Landauer R 1999 *Rev. Mod. Phys.* **71** S306
[8] Tao N J 2006 *Nat. Nanotechnol.* **1** 173–81
[9] Venkataraman L, Klare J E, Tam I W, Nuckolls C, Hybertsen M S and Steigerwald M L 2006 *Nano Lett.* **6** 458–62
[10] Smit R H M, Noat Y, Untiedt C, Lang N D, van Hemert M C and van Ruitenbeek J M 2002 *Nature* **419** 906–9
[11] Čermák J, Rezek B, Cimrová V, Výprachtický D, Ledinský M, Mates T, Fejfar A and Kočka J 2007 *Phys. Status Solidi (RRL)* **1** 193–5
[12] Forest S R 2004 *Nature* **428** 911
[13] Street G B 1986 *Handbook of Conducting Polymers* vol 1 (New York: Dekker) pp 265–91
[14] Lee A, Peteu S F, Ly J V, Requicha A A G, Thompson M E and Zhou C 2008 *Nanotechnology* **19** 165501
[15] Smela E 1999 *J. Micromech. Microeng.* **9** 1–18
[16] Rezek B, Čermák J, Kromka A, Ledinský M and Kočka J 2009 *Diamond Relat. Mater.* **18** 249–52
[17] John R K and Kumar D S 2002 *J. Appl. Polym. Sci.* **83** 1856–9
[18] Brédas J L, Thémans B, Fripiat J G, André J M and Chance R R 1984 *Phys. Rev.* B **29** 6761
[19] Micaroni L, Nart F C and Hümmelgen I A 2002 *J. Solid State Electrochem.* **7** 55–9
[20] Yun M, Myung N V, Vasquez R P, Lee C, Manke E and Penner R M 2004 *Nano Lett.* **4** 419
[21] Čermák J, Rezek B, Kromka A, Ledinský M and Kočka J 2009 *Diamond Relat. Mater.* **18** 1098–101
[22] Rezek B, Čermák J, Ledinský M and Kočka J 2009 private communication
[23] Shen J, Chen Z, Wang N, Yan H, Shi G, Jin A and Gu C 2006 *Appl. Phys. Lett.* **88** 253106
[24] Gence L, Faniel S, Gustin C, Melinte S, Bayot V, Callegari V, Reynes O and Demoustier-Champagne S 2007 *Phys. Rev.* B **76** 115415
[25] Sankey O F and Niklewski D J 1989 *Phys. Rev.* B **40** 3979–95
[26] Demkov A A, Ortega J, Sankey O F and Grumbach M P 1995 *Phys. Rev.* B **52** 1618–30
[27] Lewis J P, Glaesemann K R, Voth G A, Fritsch J, Demkov A A, Ortega J and Sankey O F 2001 *Phys. Rev.* B **64** 195103
[28] Jelínek P, Wang H, Lewis J P, Sankey O F and Ortega J 2005 *Phys. Rev.* B **71** 235101–9
[29] Basanta M A, Dappe Y J, Jelínek P and Ortega J 2007 *Comput. Mater. Sci.* **39** 759–66
[30] Kohn W and Sham L J 1965 *Phys. Rev.* **140** A1133–8
[31] Monkhorst H J and Pack J D 1976 *Phys. Rev.* B **13** 5188
[32] Vázquez H, Oszwaldowski R, Pou P, Ortega J, Pérez R, Flores F and Kahn A 2004 *Europhys. Lett.* **65** 802–8
[33] Čermák J, Kromka A, Ledinský M and Rezek B 2009 *Diamond Relat. Mater.* **18** 800–3
[34] Tomfohr J K and Sankey O F 2002 *Phys. Rev.* B **65** 245105
[35] Lee M H, Speyer G and Sankey O F 2007 *J. Phys.: Condens. Matter* **19** 215204
[36] Kümmel S and Kronik L 2008 *Rev. Mod. Phys.* **80** 3
[37] Sau J D, Neaton J B, Choi H J and S G Louie M L C 2008 *Phys. Rev. Lett.* **101** 026804
[38] Marom N, Hod O, Scuseria G E and Kronik L 2008 *J. Chem. Phys.* **128** 164107
[39] Vázquez H, Jelínek P, Brandbyge M, Jauho A P and Flores F 2009 *Appl. Phys.* A **95** 257–63
[40] Jelínek P, Pérez R, Ortega J and Flores F 2004 *Surf. Sci.* **556** 13–23
[41] Mingo N, Jurczyszyn L, Garcia-Vidal F J, Saiz-Pardo R, de Andreas P L, Flores F, Wu S Y and More W 1996 *Phys. Rev.* B **54** 2225
[42] Jelínek P, Pérez R, Ortega J and Flores F 2003 *Phys. Rev.* B **68** 085403
[43] Jelínek P, Pérez R, Ortega J and Flores F 2005 *Nanotechnology* **16** 1023–8